ORIGINAL RESEARCH

Susceptibility-Weighted MR Imaging for Diagnosis of Capillary Telangiectasia of the Brain

M. El-Koussy
G. Schroth
J. Gralla
C. Brekenfeld
R.H. Andres
S. Jung
M.A. Shahin
K.O. Lovblad
C. Kiefer
R. Kottke

BACKGROUND AND PURPOSE: BCT is a benign entity, whose appearance on conventional MR imaging makes its differentiation from neoplastic, inflammatory, or subacute ischemic disease challenging. SWI is sensitive to susceptibility effects from deoxyhemoglobin with excellent spatial resolution. Only scarce case reports have described the utility of SWI in cases of BCT. Our aim was to show the diagnostic value of SWI applied to a larger series of cases.

MATERIALS AND METHODS: This was an observational retrospective study of 33 BCTs in 27 consecutive patients examined from August 2009 to January 2011 with MR imaging, including SWI. Morphology, signal intensity characteristics, and additional vascular malformations were analyzed. Preceding or follow-up examinations were available in 18 patients with a median time interval of 14.5 months (range, 2–115 months).

RESULTS: Twenty-five pontine and 8 supratentorial BCTs demonstrated distinct signal-intensity loss on SWI in combination with postcontrast enhancement. Mean lesion diameter was 4.9 mm (range, 1.5–17 mm). Thirty-nine percent showed slight signal-intensity changes on T1 and/or T2; the remainder were isointense to normal brain. In 30%, a prominent draining vessel was observed. Additional cerebral vascular malformations were found in 5 patients.

CONCLUSIONS: SWI represents a valuable tool for confirmation of presumed BCT. Demonstration of signal-intensity loss on SWI in an enhancing focal brain lesion, otherwise unremarkable on conventional MR images, is highly specific for BCT, thus excluding serious pathology and reassuring the patient and referring physician. This is particularly helpful for BCT in less typical locations.

ABBREVIATIONS: BCT = brain capillary telangiectasia; DVA = developmental venous anomaly; GRE = gradient-recalled echo

BRAIN

ORIGINAL RESEARCH

BCT is usually an incidental finding on MR imaging of the brain. It is considered a benign entity, generally asymptomatic and without further implications for patient management. BCT is inconspicuous on conventional precontrast MR images and in most cases is detected due to faint enhancement after intravenous gadolinium administration. Thus BCT may be confused with serious pathology, including neoplastic, inflammatory, or subacute ischemic disease, resulting in unnecessary follow-up imaging, surgical biopsy, or even instigation of treatment for presumed pathology.[1]

In 1996 and 1997, two publications described the value of the T2*-GRE technique to diagnose BCT by a local loss of MR imaging signal intensity.[1,2] This is explained by low-velocity blood flow in ectatic venous channels of a BCT, resulting in a drop of oxygen saturation of hemoglobin increasing the local deoxyhemoglobin levels and causing the observed susceptibility effect. SWI has been recently implemented in clinical MR imaging. It is known to be more sensitive to susceptibility changes than 2D T2*-GRE[3] and is able to demonstrate small BCTs that are not detected on T2*-GRE images.[4] So far, only 2 single case reports have been published on the diagnosis of BCT by using SWI.[5,6] One case showed the superior sensitivity of SWI compared with T2*-GRE imaging for a pontine BCT in a patient with suspected neoplastic disease.[6] With higher sensitivity and superior resolution compared with T2*-GRE, SWI seems to be ideally suited to confirm the diagnosis of BCT. Our aim was to demonstrate this diagnostic potential of SWI in a larger series of patients with BCT.

Received May 11, 2011; accepted after revision June 23.

From the Institute of Diagnostic and Interventional Neuroradiology (M.E.-K., G.S., J.G., C.B., C.K., R.K.), Departments of Neurosurgery (R.H.A.) and Neurology (S.J.), University Bern, Inselspital, Bern, Switzerland; Department of Radiology (M.A.S., M.E.-K.), Cairo University Hospitals, Kasr Al Aini, Cairo, Egypt; and Department of Neuroradiology (K.O.L.), University Geneva, Geneva, Switzerland.

Please address correspondence to Marwan El-Koussy, MD, Institute of Diagnostic and Interventional Neuroradiology, University Bern, Inselspital, Freiburgstr 4, 3010 Bern, Switzerland; e-mail: marwan.el-koussy@insel.ch

Indicates article with supplemental on-line tables.

http://dx.doi.org/10.3174/ajnr.A2893

Materials and Methods

Subjects

For this observational retrospective study, we screened 6399 contrast-enhanced MR studies of the brain that were performed in our institution from August 2009, coinciding with the implementation of SWI on our clinical MR scanners, until January 2011. Lesions consistent with BCT were diagnosed in 43 patients. Of these, 27 patients (9 males, 18 females; age range, 6–86 years; mean age, 51 years; median age, 44 years) received SWI in addition to the gadolinium-enhanced images and were included into the study. In these 27 patients, 33 enhancing lesions met the diagnostic criteria for BCT (On-line Table 1). Preceding or follow-up examinations, including contrast-enhanced images, were available in 18/27 patients with a median time interval of 14.5 months (range, 2–115 months). None of the patients underwent biopsy or surgical resection of the BCT.

MR Imaging

MR imaging was performed on 1.5T and 3T MR scanners (Magnetom Avanto and Magnetom Verio, respectively; Siemens, Erlangen, Germany) equipped with a 32-channel and 12-channel head coil, respectively. Thirteen patients were examined at 1.5T and 14 patients at 3T.

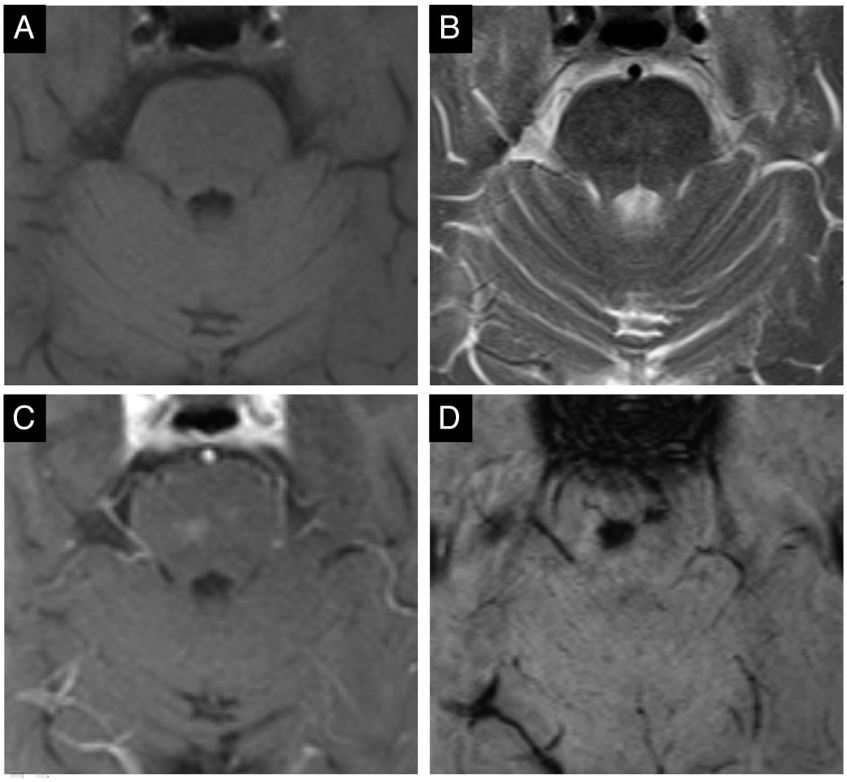

Fig 1. Typical case of 2 pontine BCTs (case 4). Isointense on T1- (*A*), slightly hyperintense on T2-weighted images (*B*), faint homogeneous enhancement after gadolinium (*C*), and considerable signal intensity drop on SWI (*D*).

Standard MR imaging protocol comprised axial spin-echo T2- and T1-weighted images, DWI, FLAIR, postcontrast axial spin-echo T1, and 3D-T1-GRE images. Intravenous gadobutrol (Gadovist 1.0; Bayer-Schering Pharma, Berlin, Germany) was administered at a concentration of 0.1 mmol/kg.

SWI was performed before gadolinium administration in all patients except 1 (case 7). Scanning parameters were the following: at 1.5T, TR/TE, 49/40 ms; FOV, 230 mm; matrix size, 320 × 208; voxel size, 0.9 × 0.7 × 1.8 mm; flip angle, 15°; and at 3T, TR/TE, 28/20 ms; FOV, 230 mm; matrix, 320 × 168; voxel size, 1.0 × 0.7 × 1.2 mm; flip angle, 15°. Minimum intensity projections were generated automatically by the scanner software. In 5 patients, axial 2D-T2*-GRE images (TR, 620 ms; TE, 19.9 ms; section thickness, 5 mm; FOV, 192 × 220 mm) were acquired. Whole-brain DWI included 19 axial images with $b = 0$ and $b = 1000$ values. At 1.5T, we used the following parameters: TR/TE, 2600/82 ms; section thickness, 5 mm; FOV, 230 mm; matrix size, 192 × 192. The parameters at 3T were the following: TR/TE, 5500/98 ms; FOV, 230 mm; matrix size, 128 × 128. ADC maps were automatically calculated.

Image Analysis

In accordance with established diagnostic criteria, a focal lesion was considered consistent with BCT if it displayed the following characteristics: isointense or slightly hyperintense on T2, and isointense or slightly hypointense on T1-weighted images, mild postgadolinium enhancement, signal-intensity loss on T2*-GRE images and/or SWI, no mass effect or architectural distortion of adjacent parenchyma, and no interval change on follow-up examinations (Fig 1).[1,2,7,8] The MR images were interpreted in consensus reading by 2 board-certified radiologists (M.E.K., R.K.) with 16 and 8 years of experience, respectively. The presence of prominent draining vessels or additional vascular malformations was documented.

Results

Clinical Indications for MR Imaging

The clinical presentation and/or suspected diagnosis in 15/27 patients included migraine ($n = 4$), transient ischemic attack ($n = 2$), acute ischemia ($n = 4$), right facial dysesthesia and headache ($n = 1$), slowly progressive aphasia without evidence of acute ischemia on MR imaging ($n = 1$), fluctuating sensorineural hearing loss ($n = 1$), cognitive deficits/dementia ($n = 1$), and cranial nerve palsy ($n = 1$) (On-line Table 1). The neurologic symptoms were not attributed to the BCTs. In the remaining 12 patients, MR imaging was performed as follow-up examination for a known pathology. In 4 patients (cases 4, 13, 17, and 22), MR imaging was requested to further characterize or follow-up an enhancing lesion in the left insular region (case 13) and in the pons (cases 4, 17, and 22).

Imaging Findings

Thirty-three lesions, 25 (76%) infratentorial and 8 (24%) supratentorial, consistent with BCT, were identified in 27 patients. All infratentorial BCTs were located in the pons. Supratentorial BCTs were found in the frontal lobe (cingulate gyrus, $n = 2$; insula, $n = 1$; substantia innominata, $n = 1$), basal ganglia ($n = 3$), and occipital white matter ($n = 1$) (On-line Table 2). Multiple BCTs were seen in 4 patients (12%): Case 1 showed 3 pontine lesions and 1 in the left frontal lobe; cases 3, 4, and 22 had 2 pontine BCTs each. Most BCTs were small,

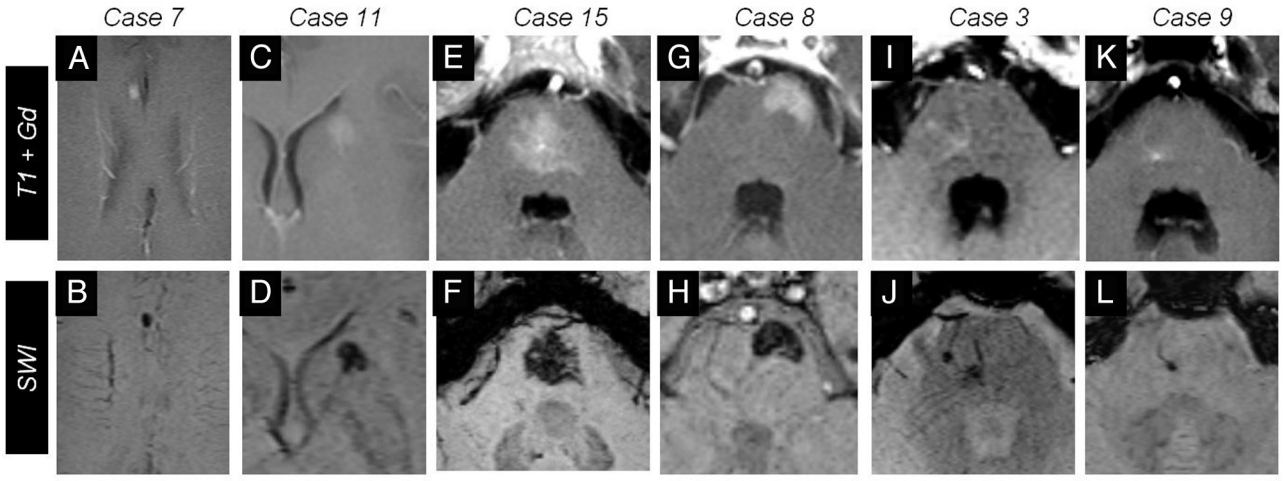

Fig 2. Six representative cases of BCTs on gadolinium-enhanced (upper row) and SWI images (lower row). *A–D*, Cases 7 and 11 show supratentorial BCTs. Notice the signal intensity drop on SWI in case 7 (*B*) and the BCT in the head of caudate in case 11 (*C*). Four cases of infratentorial BCTs are presented. *E–H*, Cases 15 and 8 present rather large BCTs: a central pontine BCT with irregular brushlike borders (*E* and *F*) and a superficial, left ventrolateral pontine BCT in case 8 (*G* and *H*). *I–L*, Cases 3 and 9 are smaller BCTs of the pons. Note that SWI more clearly depicts the prominent vessel pointing to the BCT.

with an average maximum diameter on postcontrast images of 4.9 mm (median, 4 mm; range, 1.5–17 mm). Seven of 33 BCTs (21%) measured >5 mm; only 3 lesions (9%) were >10 mm (cases 8, 15, and 20). Measurements on SWI images (mean, 5.2; median, 4.5; range, 1.5–18 mm) were very similar to the values obtained on postcontrast images. In 10 BCTs (30%), a prominent draining vessel was seen on SWI, postcontrast T1-weighted images, and GRE images, independent of lesion diameter (mean, 5 mm; median, 4 mm; range, 2–11 mm) (Online Table 2).

A total of 13/33 (39%) BCTs exhibited slight signal-intensity abnormalities on precontrast T1, T2, and/or FLAIR images; the remaining were undetectable. On T1-weighted images, 8 BCTs (24%) could hardly be seen, being slightly hypointense. On T2-weighted images, 8 lesions (24%) were slightly hyperintense. On FLAIR images, which were available for 18 patients (24 BCTs), 20 BCTs were isointense to adjacent parenchyma, while 4 lesions were slightly hyperintense (Online Table 2).

On DWI (b = 1000 image), available in 25/27 patients (31/33 lesions), 14 BCTs were hypointense. Fifteen BCTs were not visualized, being isointense or too small, while in 2 cases, artifacts prevented evaluation. Of 22 pontine BCTs, 10 lesions (46%) showed hypointense signal intensity on DWI. Of the 6 supratentorial BCTs, 4 lesions (67%) showed hypointense signal intensity on DWI. ADC maps showed corresponding high signal intensity in only 6 of the 14 BCTs detectable on DWI. The 3 largest BCTs (cases 8, 15, and 20) were visualized on T1- (except case 20) and T2-weighted images as well as on DWI. On the ADC map, 1 lesion was hyperintense. Due to artifacts from the skull base or movement, corresponding sections were considered not diagnostic in 2 cases for DWI and 7 cases with the ADC map.

After intravenous gadolinium, all 33 BCTs enhanced. The smallest lesions presented as focal spots of enhancement. Larger BCTs showed faint-to-moderate homogeneous enhancement with ill-defined irregular borders, in some cases with weblike linear enhancement, possibly representing slightly larger vascular channels of the BCT. On postgadolinium isotropic thin-section 3D-GRE T1-weighted images, lesion structure was seen more clearly in several cases, though enhancement in some of the smaller lesions was more difficult to appreciate.

On SWI, all 33 BCTs showed homogeneous marked (n = 31) or moderate (n = 2) signal-intensity loss. Good contrast and demarcation of the lesions was observed. In all cases, the configuration of the BCT was similar to that seen on postcontrast T1- and T2*-GRE (when available) images (Fig 2). There was no relevant difference in image quality or signal intensity of the BCTs examined at 1.5T compared with 3T.

Additional T2*-GRE images were available in 5 patients. In cases 1 and 9, no lesion was detectable on 2 different studies at 1.5T; in case 22, two pontine BCTs were detectable on MR imaging at 3T but not at 1.5T. In 2 cases, BCT was seen on T2*-GRE at 3T (cases 8 and 13) (Fig 3).

In 1 patient (case 4), single-voxel spectroscopy of a pontine BCT was performed with good quality of spectra showing only water signal intensity; no concentrations of *N*-acetylaspartate, choline, or creatine were registered.

Additional cerebral vascular malformations were observed in 5 subjects. Case 1 had a large cavernous angioma of the basal ganglia with an adjacent DVA. Four patients had a DVA (cases 5, 21, 23, and 24). There was no close spatial relation between these malformations and the BCT.

On preceding and consecutive examinations, which were available for 18/27 patients, the size, configuration, signal intensity, and degree of enhancement of BCT remained unchanged in all patients and sequences. Follow-up imaging, including SWI, was only available in 3 patients (cases 9, 17, and 18). In 2 patients (case 3 and 9), 3 pontine BCTs were also visible on contrast-enhanced CT studies of the brain.

In the 18-month period of this study, a total of 6399 contrast-enhanced MR imaging studies of the brain were performed in our institution. Lesions consistent with BCT were diagnosed in 43 patients, corresponding to a prevalence of 0.67% in this collective of patients.

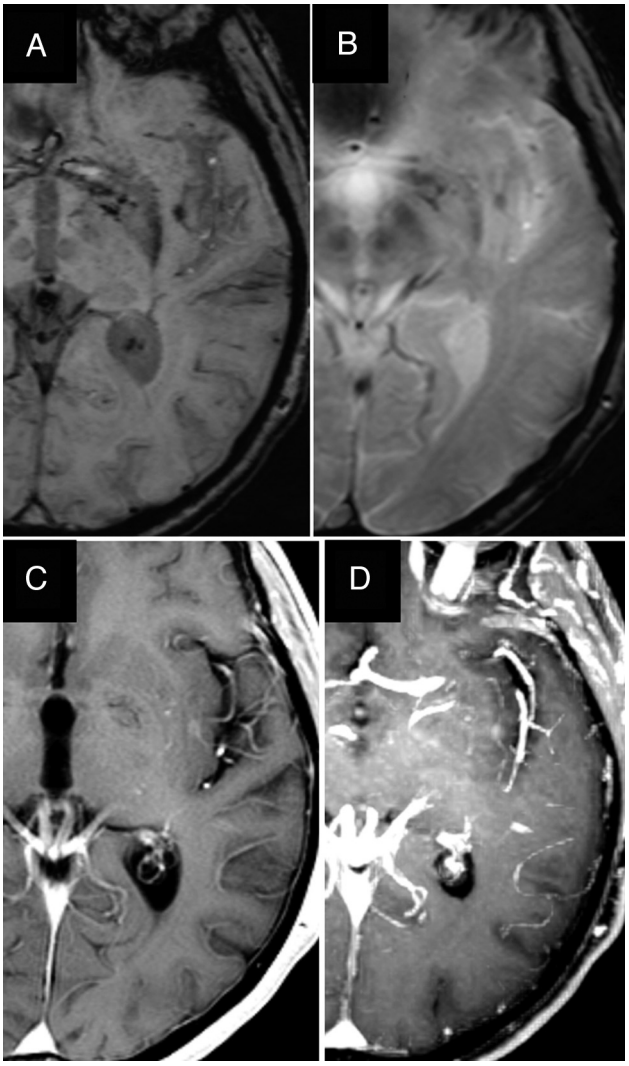

Fig 3. BCT in the left insular region (case 13). The BCT and the adjacent prominent vessels anterior and posterior to it are more clearly seen on SWI (*A*) compared with T2*-GRE (*B*). Axial enhanced image (*C*) and reconstructed maximum-intensity-projection (MIP) image (*D*) depict the BCT and prominent vessels, though they are better seen on the MIP image.

Discussion

Cerebral vascular malformations include AVM, DVA, cavernous angioma, and BCT. AVM, DVA, and cavernous angioma are usually readily diagnosed on conventional MR images. BCT is a low-flow angiographically occult malformation. It accounts for ≤10% of all intracerebral vascular malformations and is considered the second most common vascular malformation of the central nervous system after DVA.[9-12] An estimated prevalence at postmortem examination of 0.4%–0.7% has been reported,[11,12] which is similar to the prevalence of 0.67% we observed in our 18-month study interval.

In our collective, we examined a total of 33 BCTs. The mean size was 0.5 cm (range, 0.2–1.7 cm), which corresponds to values given in the literature (0.3–2 cm).[1,2,7] BCT is generally considered a benign entity; only sporadic cases of symptomatic lesions have been described.[13-15] Symptoms may be related to the size of the lesion. In a study by Sayama et al,[9] 7/105 BCTs (6.7%) were >1 cm; 2 of these lesions (28.6%) were identified as likely causing symptoms. In our series, 3 lesions (9%) were >1 cm. No symptoms could be attributed to the BCTs.

One of the first descriptions of capillary telangiectasia was in 1941 by Blackwood,[16] who published 2 cases of histologically proved BCT. Histologically, this malformation consists of dilated capillaries with interspersed normal brain tissue. Gliosis, calcification, or hemosiderin deposition are not observed. On contrast-enhanced CT scans, a BCT is rarely detected, depending on the size and location. A small BCT of the pons is most often missed on CT due to bone-hardening artifacts in the posterior fossa. On conventional precontrast MR imaging, a BCT is inconspicuous, being isointense or slightly hyperintense to healthy brain tissue on T2- and iso- or slightly hypointense on T1-weighted images. After gadolinium administration, a BCT typically demonstrates mild-to-moderate enhancement with irregular brushlike borders. Differentiation from a neoplasm, subacute infarction, or inflammatory disease can be impossible on a single MR imaging examination. Consequences may include inappropriate therapy, surgical biopsy, or follow-up examinations causing distress to patients.[1,9]

To avoid the diagnostic dilemma, a characteristic signal-intensity loss on susceptibility-sensitive T2*-GRE sequences has been described, which, in conjunction with postcontrast enhancement, is virtually diagnostic of BCT (On-line Table 3).[1,2] It is thought that slow-velocity blood-flow in the ectatic venous channels results in MR imaging signal-intensity loss owing to the paramagnetic effect of deoxyhemoglobin. This effect is not strong enough to be observed on conventional spin-echo T2-weighted images.[1]

SWI, originally called high-resolution blood oxygenation level–dependent venography, was initially developed for MR venography without extrinsic contrast agent exploiting the paramagnetic effect of intravascular deoxyhemoglobin.[4,17,18] On the basis of high-resolution 3D-GRE sequences with long TEs, SWI combines phase and magnitude information. Through multiplication of a phase-mask with the magnitude image, excellent contrast at submillimeter resolution is achieved. SWI is extremely sensitive for susceptibility dephasing from deoxyhemoglobin, iron, calcium, and hemosiderin. SWI is used for the diagnosis of cerebral microbleeds and hemorrhagic shearing injuries and for iron imaging in neurodegenerative disease. It is also well-suited for depicting slow-flow vascular malformations like BCT or cavernous angioma.

Lee et al[4] reported 2 cases of presumed BCT, which were visible on high-resolution blood oxygenation level–dependent venography but were not detectable on T2*-GRE images. Yoshida et al[6] reported a patient infected with human T-cell leukemia virus type 1 with suspected T-cell leukemia. MR imaging demonstrated a small enhancing pontine lesion not visible on T2*-GRE; however, its SWI hypointensity confirmed the diagnosis of BCT, excluding neoplastic manifestation. A follow-up MR imaging 7 months later showed no interval change. In our series, T2* GRE sequences were available in 8 MR studies, acquired in 5 patients with 9 lesions consistent with BCT. In 4 of 8 MR imaging studies, 7 lesions were not detected on T2*-GRE images, whereas they were apparent on SWI, indicative of the inferior sensitivity of T2*-GRE. This can be partly explained by the larger section thickness of T2*-GRE images.

Thirty-nine percent of BCTs examined in this study showed slight signal-intensity changes on either T1, T2, or FLAIR sequences. The remainder would be easily missed, being isointense to healthy parenchyma. All lesions demonstrated mild-to-moderate enhancement with irregular and brushlike borders without mass effect. Corresponding signal-intensity loss was seen in all lesions on SWI. Signal-intensity loss was marked in 31 lesions and moderate in 2 lesions, correlating with weak enhancement. A prominent draining vein was depicted in 30% (10/33) of lesions, independent of lesion size. As early as 1941, prominent collecting veins in BCT have been reported. A decrease in the total number of draining veins with dilation of the central draining veins was described.[16] This is probably reflected on postcontrast MR imaging as a weblike pattern with small linear enhancing structures in some large BCTs. Associated vascular malformations have been described. It is possible that symptoms attributed to "symptomatic" BCTs are actually caused by undetected coexisting small cavernous angiomas.[12,19-22] In our collective, additional vascular malformations were found in 15% of cases, mainly DVA, but not in close spatial relation to the BCT.

In a series of 18 pontine BCTs, all lesions displayed low signal intensity on DWI. Thus DWI was suggested as a highly sensitive tool in the diagnosis of such cases. Information with respect to lesion size was not given.[23] In contrast, <50% of BCTs in our collective were detectable on DWI, showing hypointense signal intensity. Only 46% of pontine BCTs were hypointense on DWI. Sensitivity for supratentorial lesions seems to be better because 67% (4/6) of examined lesions were detectable on DWI; however, the limited number of cases does not allow a definite conclusion. Hypointense signal intensity on DWI, if present, can be used, especially for larger and supratentorial BCTs for additional information when SWI is not available.

We found only 2 large series including supratentorial BCTs examined with MR imaging (On-line Table 3).[1,9] In our series, 24% of BCTs were detected in the cerebral hemispheres, indicating that a supratentorial location may not be that uncommon after all. Castillo et al[24] reported a case of a large BCT of the basal ganglia, which was diagnosed after stereotactic biopsy. Most supratentorial BCTs previously mentioned in the literature were located in the basal ganglia.[1,9,24] There may be a predilection for the basal ganglia because most of our supratentorial BCTs were seen close to or in the basal ganglia. It is also possible that these are less easily overlooked than those in a more peripheral location. Histologic material was not available in our study, but MR imaging was characteristic for BCT with no interval change on follow-up examinations.

Refinement of MR imaging techniques in recent years, including improved spatial resolution of postcontrast sequences, has increased the number of BCTs detected.[24] This may pose a diagnostic problem in the future if susceptibility-sensitive sequences are not used or are not sensitive enough. BCT is often only detected after administration of gadolinium. In this case, the imaging protocol can easily be extended with SWI. No image-quality degradation or relevant signal-intensity change compared with precontrast SWI is to be expected as has recently been shown in a study comparing SWI before and after gadolinium administration.[25]

A limitation of our study, as in previous publications, is the lack of histopathologic confirmation. Due to the benign nature of BCT and the characteristic MR imaging features, the histopathologic material from biopsy or excision is not available. Also, no relation between the BCT and presenting symptoms in the patients with neurologic symptoms could be found. Possible differentials for a focal contrast-enhancing lesion like subacute infarction or inflammatory or neoplastic processes could be excluded with high certainty. Follow-up studies were not available in all patients; if imaging was characteristic for BCT, a follow-up scan for confirmation was not considered necessary. A further limitation is that owing to the retrospective data collection, T2*-GRE sequences for comparison were only available in a minority of cases. The physical properties of SWI and T2*-GRE have been well documented in literature so that SWI has largely replaced T2*-GRE imaging in our institution. The observed prevalence of BCT should be considered as biased because it was calculated from a selected patient group examined at a single institution.

Conclusions

We present a larger series of pontine and supratentorial BCTs. The combination of signal-intensity loss on SWI and focal enhancement in a lesion otherwise unremarkable on conventional MR images is virtually diagnostic for BCT and serves to discard serious differential diagnoses with high specificity, reassuring patients and referring physicians. This is particularly helpful for BCT in atypical locations. SWI is extremely sensitive to susceptibility effects and offers high spatial resolution and excellent contrast. It can replace T2*-GRE imaging in such cases and can be amended after contrast-enhanced images.

Disclosures: Jan Gralla—*UNRELATED: Consultancy*: ev3, *Comments*: principal investigator of the Solitaire FR Thrombectomy for Acute Revascularisation trial, *Travel/Accommodations/Meeting Expenses*: ev 3. Karl-olaf Lovblad-*UNRELATED: Grants/Grants Pending*: Bayer Schering.* Gerhard Schroth—*UNRELATED: Grants/Grants Pending/Payment for Lectures (including service on Speakers Bureaus)*: Siemens,* Bayer Schering,* Bracco;* *Comments*: Companies support the university institute by paying partial salary and material for developing new techniques for diagnosis and treatment of stroke; none of this support has any connection with SWI MR imaging. * Money paid to institution.

References

1. Lee RR, Becher MW, Benson ML, et al. **Brain capillary telangiectasia: MR imaging appearance and clinicohistopathologic findings.** *Radiology* 1997;205:797–805
2. Barr RM, Dillon WP, Wilson CB. **Slow-flow vascular malformations of the pons: capillary telangiectasias?** *AJNR Am J Neuroradiol* 1996;17:71–78
3. Haacke EM, Mittal S, Wu Z, et al. **Susceptibility-weighted imaging: technical aspects and clinical applications, part 1.** *AJNR Am J Neuroradiol* 2009;30:19–30
4. Lee BC, Vo KD, Kido DK, et al. **MR high-resolution blood oxygenation level-dependent venography of occult (low-flow) vascular lesions.** *AJNR Am J Neuroradiol* 1999;20:1239–42
5. Pendharkar HS, Thomas B, Gupta AK. **Susceptibility-weighted imaging in capillary telangiectasia.** *Neurol India* 2010;58:618–19
6. Yoshida Y, Terae S, Kudo K, et al. **Capillary telangiectasia of the brain stem diagnosed by susceptibility-weighted imaging.** *J Comput Assist Tomogr* 2006;30:980–82
7. Auffray-Calvier E, Desal HA, Freund P, et al. **Capillary telangiectasis, angiographically occult vascular malformations. MRI symptomatology apropos of 7 cases** [in French]. *J Neuroradiol* 1999;26:257–61
8. Küker W, Nacimiento W, Block F, et al. **Presumed capillary telangiectasia of the pons: MRI and follow-up.** *Eur Radiol* 2000;10:945–50
9. Sayama CM, Osborn AG, Chin SS, et al. **Capillary telangiectasias: clinical, radiographic, and histopathological features—Clinical article.** *J Neurosurg* 2010;113:709–14
10. Chaloupka JC, Huddle DC. **Classification of vascular malformations of the central nervous system.** *Neuroimaging Clin N Am* 1998;8:295–321

11. Jellinger K. **Vascular malformations of the central nervous system: a morphological overview.** *Neurosurg Rev* 1986;9:177–216
12. Sarwar M, McCormick WF. **Intracerebral venous angioma: case report and review.** *Arch Neurol* 1978;35:323–25
13. Beukers RJ, Roos YB. **Pontine capillary telangiectasia as visualized on MR imaging causing a clinical picture resembling basilar-type migraine: a case report.** *J Neurol* 2009;256:1775–77
14. Kapnadak SG, Mikolaenko I, Enfield K, et al. **Ondine's curse with accompanying trigeminal and glossopharyngeal neuralgia secondary to medullary telangiectasia.** *Neurocrit Care* 2010;12:395–99
15. Scaglione C, Salvi F, Riguzzi P, et al. **Symptomatic unruptured capillary telangiectasia of the brain stem: report of three cases and review of the literature.** *J Neurol Neurosurg Psychiatry* 2001;71:390–93
16. Blackwood W. **Two cases of benign cerebral telangiectasis.** *J Pathol Bact* 1941;52:209–13
17. Reichenbach JR, Essig M, Haacke EM, et al. **High-resolution venography of the brain using magnetic resonance imaging.** *MAGMA* 1998;6:62–69
18. Reichenbach JR, Venkatesan R, Schillinger DJ, et al. **Small vessels in the human brain: MR venography with deoxyhemoglobin as an intrinsic contrast agent.** *Radiology* 1997;204:272–77
19. Abla A, Wait SD, Uschold T, et al. **Developmental venous anomaly, cavernous malformation, and capillary telangiectasia: spectrum of a single disease.** *Acta Neurochir (Wien)* 2008;150:487–89, discussion 489
20. Bonneville F, Cattin F, Bonneville JF. **The juxtaposition of a capillary telangiectasia, cavernous malformation, and developmental venous anomaly in the brainstem of a single patient: case report.** *Neurosurgery* 2002;51:850–51, author reply 851
21. Clatterbuck RE, Elmaci I, Rigamonti D. **The juxtaposition of a capillary telangiectasia, cavernous malformation, and developmental venous anomaly in the brainstem of a single patient: case report.** *Neurosurgery* 2001;49:1246–50
22. Pozzati E, Marliani AF, Zucchelli M, et al. **The neurovascular triad: mixed cavernous, capillary, and venous malformations of the brainstem.** *J Neurosurg* 2007;107:1113–19
23. Finkenzeller T, Fellner FA, Trenkler J, et al. **Capillary telangiectasias of the pons: does diffusion-weighted MR increase diagnostic accuracy?** *Eur J Radiol* 2010;74:e112–16
24. Castillo M, Morrison T, Shaw JA, et al. **MR imaging and histologic features of capillary telangiectasia of the basal ganglia.** *AJNR Am J Neuroradiol* 2001;22:1553–55
25. El-Koussy M, Schenk P, Kiefer C, et al. **Susceptibility-weighted imaging of the brain: does gadolinium administration matter?** *Eur J Radiol* 2012;81:272–76